An Enhanced Tilted-Angle Acoustofluidic Chip for Cancer Cell Manipulation

Fangda Wu, Ming Hong Shen, Jian Yang, Hanlin Wang, Roman Mikhaylov, Aled Clayton, Xinghua Qin, Chao Sun, Zhihua Xie, Meng Cai, Jun Wei, Dongfang Liang, Fan Yuan, Zhenlin Wu, Yongqing Fu, Zhiyong Yang, Xianfang Sun, Liangfei Tian, Xin Yang

***Abstract*—In recent years, surface acoustic wave (SAW) devices have demonstrated great potentials and increasing applications in the manipulation of nano- and micro-particles including biological cells with the advantages of label-free, high sensitivity and accuracy. In this letter, we introduce a novel tilted-angle SAW devices to optimise the acoustic pressure inside a microchannel for cancer-cell manipulation. The SAW generation and acoustic radiation force are improved by seamlessly patterning electrodes in the space surrounding the microchannel. Comparisons between this novel SAW device and a conventional device show a 32% enhanced separation efficiency while the input power, manufacturing cost and fabrication effort remain the same. Effective separation of HeLa cancer cells from peripheral blood mononuclear cells is demonstrated. This novel SAW device has the advantages in minimizing device power consumption, lowering component footprint and increasing device density.**

***Index Terms*—Surface acoustic wave (SAW), cancer cells, acoustofluidics, acoustic separation.**

I. Introduction

ACOUSTOFLUIDIC devices are essential tools for label-free and contactless manipulations of biological samples for point-of-care and fast disease diagnostics[1]. These devices using either bulk acoustic waves (BAWs) or surface acoustic waves (SAWs) produce an acoustic pressure gradient and streaming within a fluid, thus achieving the capability of actuating micro-/nano-particles inside. BAW-based separation devices usually employ the microchannel to be part of the system, whose operation relies on not only the acoustic transducer but also the property of the microchannel material[2]. Surface acoustic wave (SAW) based acoustofluidic devices are compact and easy to fabricate for high-frequency applications (MHz – GHz). They are versatile and less-dependent on the acoustic property of the microchannel when compared to those made using BAWs. SAW acoustofluidic devices are usually fabricated by patterning interdigital transducers (IDTs) on a piezoelectric substrate bonded with a microchannel. When a pair of IDTs with the same parameters are in use to generate counter-propagating SAWs, standing SAW (SSAW) is produced exhibiting minimum pressure area (pressure node, PN) and maximum pressure area (pressure antinode, AN) along the propagation. High-throughput manipulation of biological samples has been achieved in conventional tilted-angle (CTA) SSAW devices as shown in Fig. 1a, which presents an inclined angle between the SSAW propagation and the flow direction in the microchannel. CTA devices have been successfully applied for manipulation of biological micro- and nano-particles such as circulating tumour cells (CTCs)[3], bacteria[4], inflammatory cells[5] and extracellular vesicles [6, 7].

SSAW has the ability to remotely manipulate micro- and nano-objects with high spatial and temporal precisions via the acoustic radiation force $\boldsymbol{F}^{\mathrm{rad}}$. A faster deflection of microparticles can be achieved by increasing the $\boldsymbol{F}^{\mathrm{rad}}$ resulting in a high-throughput processing of samples. This has been realised by enhancing acoustic energy density[3, 8, 9]. For instance, the improvement of the efficiency in a SAW-based microcirculatory system has been achieved by an optimal microchannel structure[10]. An enhanced efficiency in acoustic particles focusing has been achieved by decreasing the thickness of the microfluidic device[11]. Focused[12] and unidirectional[13] IDTs achieved high accuracy and high-

This work was supported by the Natural Science Basic Research Program of Shaanxi Province (2020JQ-233); Fundamental Scientific Research of Central Universities (grant number 3102017OQD116); the Engineering and Physical Sciences Research Council (EPSRC) (EP/P002803/1 and EP/P018998/1); and the Royal Society (IEC/NSFC/170142, IE161019). *(Corresponding author: Xin Yang.)*

F. Wu, H. Wang and R. Mikhaylov and X. Yang are with the Department of Electrical and Electronic Engineering, School of Engineering, Cardiff University, Cardiff CF24 3AA, UK (e-mail: yangx26@cardiff.ac.uk).

M. Shen and J. Yang are with the Preclinical Studies of Renal Tumours Group, Division of Cancer and Genetics, School of Medicine, Cardiff University, Cardiff CF14 4XN, UK.

A. Clayton is with the Tissue Micro-Environment Group, Division of Cancer & Genetics, School of Medicine, Cardiff University, Cardiff CF14 4XN, UK.

X. Qin and C. Sun are with the School of Life Sciences, Northwestern Polytechnical University, 710072, P.R. China.

Z. Xie is with the Department of Civil Engineering, School of Engineering, Cardiff University, Cardiff CF24 3AA, UK

M. Cai and J. Wei are with the iRegene Therapeutics Co., Ltd, Wuhan, 430070, P.R. China.

D. Liang is with the Department of Engineering, University of Cambridge, Cambridge CB2 1PZ, UK.

F. Yuan is with the Department of Biomedical Engineering, School of Engineering, Duke University, NC 27708-0281, USA.

Z. Wu is with the School of Optoelectronic Engineering and Instrumentation Science, Dalian University of Technology, 116023, P.R. China.

Y. Fu is with the Faculty of Engineering and Environment, Northumbria University, Newcastle Upon Tyne, Newcastle NE1 8ST, UK.

Z. Yang is with the School of Mechanical Engineering, Tianjin University, 300072, P.R. China.

L. Tian is with the College of Biomedical Engineering and Instrument Science, Zhejiang University, 310027, P.R. China.

X. Sun is with the School of Computer Science and Informatics, Cardiff University, Cardiff CF24 3AA, UK.

throughput separation of micro- and nano-particles. A flow divider in a microchannel streamlined with a glass-SAW device offered effective CTC sorting from the whole blood of prostate cancer patients with a considerably high throughput [3]. In addition, a high sample flow rate of up to 500 µl/min was achieved for microparticle separation by applying a novel sheathless microchannel[9]. When the mechanical properties of the micro-objects are given, i.e., their size, density and compressibility, further increase of the $\boldsymbol{F}^{\mathrm{rad}}$ is desired to speed up the manipulation process. This can be enhanced by optimising the acoustofluidic device parameters including increasing the acoustic pressure and the SAW frequency[14].

In this work, we developed a novel filled tilted-angle (FTA, Fig. 1b) SAW device for enhancing the acoustic pressure by patterning additional IDTs to fully fill the device space adjacent to the microchannel. The separation efficiency of the FTA device was investigated and compared with the CTA device. Separation of HeLa cancer cells from peripheral blood mononuclear cells (PBMCs) is successfully demonstrated at lower device input powers. This FTA has its unique advantages as an acoustofluidic device for saving the device's footprint and increasing the acoustic energy density to achieve a better manipulation performance.

II. Device Design and Fabrication

In the CTA device (Fig. 1a), a series of PN lines are formed in the SSAW field with an inclination angle θ to the liquid flow direction. The CTA device generally exhibits two zones without patterned electrodes (blue triangles in Fig. 1a), where no active SAW is generated. Our FTA device as shown in Fig. 1b redesigns the IDT pattern through extending the busbars of the electrodes towards the microchannel and patterning additional finger electrodes to occupy these zones resulting in stronger active SAW generation. The acoustic pressure p_0 of the device is accordingly increased since the device working area between the two IDTs is reduced, as the consequence of the adding electrodes, which is described by[15]:

$$p_0 = \sqrt{\alpha P_{in} \rho_s c_s / A_w}, \tag{1}$$

where α, P_{in}, ρ_s, c_s, and A_w are the power conversion factor, input power, density of the piezoelectric substrate, phase velocity of SAW, and working area, respectively. The increased p_0 enhances the $\boldsymbol{F}^{\mathrm{rad}}$ exerted on microparticles[16]. In addition, microparticles are also impeded by the Stokes drag force, $\boldsymbol{F}^{\mathrm{drag}}$, in the fluid as the inset shown in Fig. 1c[16]. The net force deflects the microparticles towards either the PNs or the ANs according to their acoustic contrast factors.

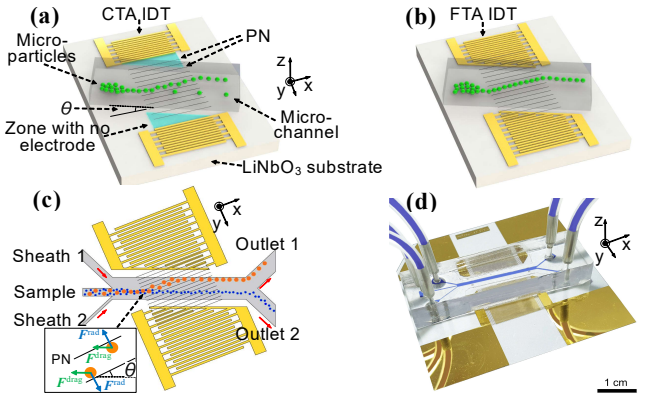

Fig. 1. The models of (a) the conventional tilted-angle (CTA) device and (b) the filled tilted-angle (FTA) device. The interdigital transducer (IDT) on the FTA device has additional electrodes to fill the blue triangle zones of the CTA. (c) The schematic illustration of the FTA separation. (d) The photo of the FTA device.

For comparative purposes, both the CTA and FTA devices were developed using similar parameters (θ=15°) except the FTA employed 24 additional finger electrodes to follow through the microchannel. The inclination angle θ relates to the samples separation distance, which was set to an optimal value i.e. θ=15° referring to the numerical simulation given in [15]. The working areas of the FTA and the CTA devices were 40 mm^2 and 70 mm^2, respectively. The 43% reduction in the working area realised by the added electrodes offers ~32% higher acoustic pressure in the FTA device (Eq.1) with the same input power. Fig. 1d shows an illustration of the FTA device, which is bonded with a microchannel made by polydimethylsiloxane (PDMS). Two sheath flows were used to focus and position the sample to enter the PN lines. The FTA has a major technical breakthrough incorporating the SAW device with microfluidics for optimising cancer cell separation. The entire FTA finger electrodes are seamlessly following through the wall of the microchannel in order to generate more effective SAW actuation while reducing the attenuation caused by the PDMS and piezoelectric substrate. A microfluidic-centered SAW device design for the enhanced separation of cancer cells is demonstrated on the FTA device. Moreover, since the FTA device employs a smaller working area (Eq. 1), to produce the same acoustic pressure requires a smaller input power resulting in reduced joule heat.

III. Results and Discussion

A. Comparisons of the FTA and CTA Devices

Numerical simulation was firstly applied to investigate the acoustic pressure on cross-sections inside the microchannel at five positions for both the FTA and CTA devices (Fig. 2a). The acoustic pressure exhibits a similar symmetric pattern at the mid-point (Position 5) of both devices (Figs. 2c & 2d). The added finger electrodes evenly follow the microchannel in the FTA device and provide equal amplitudes of the counter-propagating SAWs into the microchannel, thus the acoustic patterns in the FTA device are more uniform along the acoustic

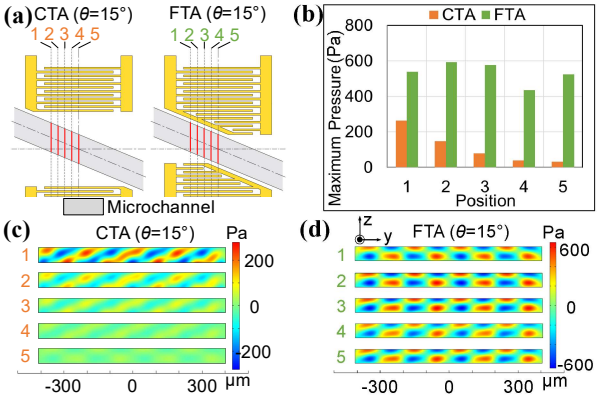

Fig. 2. (a) Five positions with the interval of 100 µm are chosen for the numerical study of the acoustic pressure in the CTA and FTA devices. (b) The maximum acoustic pressure of the five positions. (c) and (d) the acoustic pressure distribution of the five positions in the two devices.

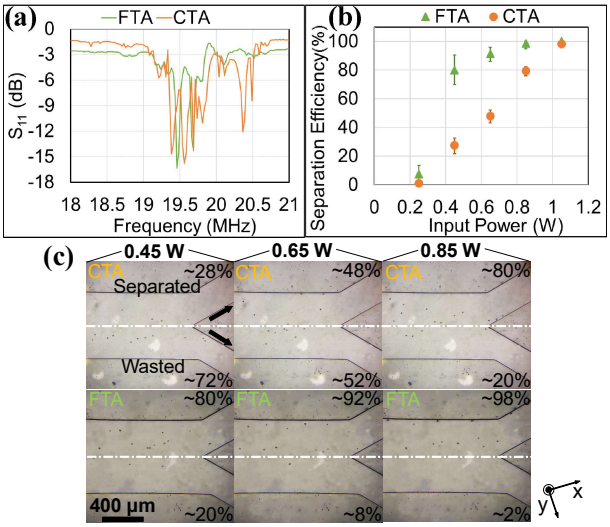

Fig. 3. (a) S_{11} of the CTA and FTA devices. (b) Separation efficiency against the input power of the two devices. (c) The microscopic image of the FTA separation at different input powers.

field, i.e., Positions 1 to 4 (Fig. 2d), while the CTA patterns vary at different positions (Fig. 2c). Moreover, the FTA offers a notably larger acoustic pressure at most positions given the same input power (Fig. 2b). The CTA's pressure is decreased from Position 1 to 4 and achieves the minimum at the mid-point (Position 5), where both the IDTs apart from the microchannel resulting in the largest attenuation. While the FTA's acoustic pressure slightly varies along the microchannel which allows more controllable manipulation of microparticles. At the entry Position 1 (Fig. 2c) where the gap between the microchannel and the lateral IDT varies the most, the acoustic pressure in the CTA shows a distorted pattern while the FTA (Fig. 2d) shows a periodic pattern, attributed to the added fingers. Details of modelling and numerical simulation in COMSOL Multiphysics with thermoviscous module can be found in SI.

The reflection coefficients (Fig. 3a), S_{11}, of both the CTA and FTA devices were measured using a vector network analyzer. The FTA device shows a better Q factor allowing a higher energy conversion. The working frequencies of the FTA and CTA devices are 19.5 MHz and 19.6 MHz, respectively. A small difference may be caused by the capacitance and inductance introduced by the added electrodes. A suspension with 15-μm polystyrene microspheres was used to evaluate the separation efficiency, W, of both the devices using $W = (c_2 V_2)/(c_1 V_1 + c_2 V_2)$. Herein, c is the microsphere concentration and V is the volume of the collection from outlets. The subscript number indicates the outlet (Fig. 1c). The microspheres were suspended in a PBS and glycerol mixture (780:176, v/v) at a concentration of 2×10^6/ml. The flow rates of the three inlets were set to allow all the microspheres to flow into Outlet 2 before applying SAW, which were 10 μl/min, 5 μl/min and 5 μl/min, respectively. The separation results are shown in Figs. 3b. The CTA device achieves 80% and 100% separations at 0.85 W and 1.05 W, respectively, which is in a good agreement with the previous studies using the CTA structure[15, 17]. The FTA shows a notably increased separation efficiency than that of the CTA in the power range. For instance, ~7% separation efficiency is achieved in the FTA device comparing with that of ~1% in the CTA at the input power of 0.25 W. The FTA achieves ~91% nearly doubling to the CTA device at the same input power of 0.65 W. Fig. 3c shows the microscopic images of the CTA and FTA devices under different input powers, where the deflection of the microspheres at the outlets are captured. Altogether, the results show that the FTA device can achieve the same separation efficiency of 80% requiring only ~57% of the CTA input power, which can reduce heat generation in the device minimizing the safety risk to biological samples and the device itself.

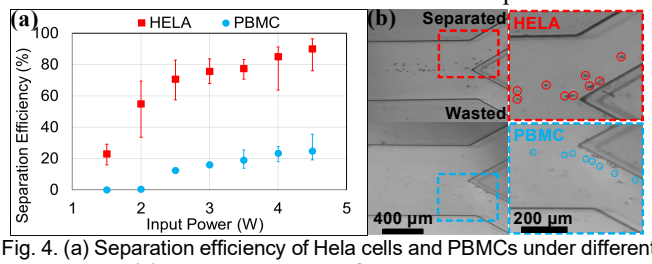

Fig. 4. (a) Separation efficiency of Hela cells and PBMCs under different input powers. (b) Microscopic image of the FTA separation at the input power of 4 W.

B. *Applying the FTA Device in Manipulation of Cancer Cells*

The FTA device has a great potential to improve the manipulation of cancer cells owing to its larger acoustic pressure created by the novel IDT structure. Commercially-sourced HeLa cells and PBMCs supplied by Cardiff University Biobank were prepared for the separation test. As the separation results shown in Fig. 4a, in general, the FTA device exhibits a higher separation efficiency on HeLa cells due to their larger, denser but less compressible yielding faster deflection than those of PBMCs[15, 18, 19]. The separation efficiencies for the HeLa cells and PBMCs are ~90% and ~25%, respectively, at the input power of 4.5 W, which allows a good separation HeLa from PBMCs while maintaining a similar cell viability of 90% as the CTA device[17]. The microscopic image displaying the cell separation at 4 W is shown in Fig. 4b, where the HeLa cells are effectively actuated and migrated to Outlet 1, whereas most PBMCs are stayed in Outlet 2. The effective manipulation of cells with an FTA device can also be applied to cell washing and patterning, blood component separation, and bacteria manipulation.

IV. Conclusion

In this letter, a novel FTA device was developed and compared with the CTA in terms of the separation efficiency. The FTA device only required a minor modification to the conventional design, i.e., adding 24 more finger electrodes to reduce the working area, without extra fabrication process and cost. The acoustic pressure was increased controllably and in a good agreement with the numerical results. A 43% reduction of the working area was achieved, which offered a significant reduction in the input power to achieve the same separation efficiency. A successful separation of HeLa cells from PBMCs was demonstrated in the FTA device. The novel device structure of the FTA had advantages in lowering energy consumption, increasing device density, and reducing device footprint.

REFERENCES

[1] M. Wu, A. Ozcelik, J. Rufo, Z. Wang, R. Fang, and T. J. Huang, "Acoustofluidic separation of cells and particles," *Microsystems & nanoengineering,* vol. 5, no. 1, p. 32 2019, DOI: 10.1038/s41378-019-0064-3

[2] N. R. Skov and H. Bruus, "Modeling of Microdevices for SAW-Based Acoustophoresis — A Study of Boundary Conditions," *Micromachines,* vol. 7, no. 10, p. 182 2016,

[3] M. Wu, P. H. Huang, R. Zhang, Z. Mao, C. Chen, G. Kemeny, P. Li, A. V. Lee, R. Gyanchandani, and A. J. Armstrong, "Circulating Tumor Cell Phenotyping via High - Throughput Acoustic Separation," *Small,* vol. 14, no. 32, p. 1801131 2018, DOI: 10.1002/smll.201801131

[4] S. Li, F. Ma, H. Bachman, C. E. Cameron, X. Zeng, and T. J. Huang, "Acoustofluidic bacteria separation," *Journal of micromechanics and microengineering : structures, devices, and systems,* vol. 27, no. 1, p. 015031 2017, DOI: 10.1088/1361-6439/27/1/015031

[5] S. Li, L. Ren, P.-H. Huang, X. Yao, R. A. Cuento, J. P. McCoy, C. E. Cameron, S. J. Levine, and T. J. Huang, "Acoustofluidic transfer of inflammatory cells from human sputum samples," *Analytical chemistry,* vol. 88, no. 11, pp. 5655-5661 2016, DOI: 10.1021/ac504330x

[6] Z. Wang, F. Li, J. Rufo, C. Chen, S. Yang, L. Li, J. Zhang, J. Cheng, Y. Kim, and M. Wu, "Acoustofluidic Salivary Exosome Isolation: A Liquid Biopsy Compatible Approach for Human Papillomavirus–Associated Oropharyngeal Cancer Detection," *The Journal of Molecular Diagnostics,* vol. 22, no. 1, pp. 50-59 2020, DOI: 10.1016/j.jmoldx.2019.08.004

[7] M. Wu, Y. Ouyang, Z. Wang, R. Zhang, P.-H. Huang, C. Chen, H. Li, P. Li, D. Quinn, M. Dao, S. Suresh, Y. Sadovsky, and T. J. Huang, "Isolation of exosomes from whole blood by integrating acoustics and microfluidics," *Proceedings of the National Academy of Sciences,* vol. 114, no. 40, p. 10584 2017, DOI: 10.1073/pnas.1709210114

[8] P. Sehgal and B. J. Kirby, "Separation of 300 and 100 nm Particles in Fabry–Perot Acoustofluidic Resonators," *Analytical Chemistry,* vol. 89, no. 22, pp. 12192-12200 2017/11/21. 2017, DOI: 10.1021/acs.analchem.7b02858

[9] M. Wu, K. Chen, S. Yang, Z. Wang, P.-H. Huang, J. Mai, Z.-Y. Li, and T. J. Huang, "High-throughput cell focusing and separation via acoustofluidic tweezers," *Lab on a Chip,* vol. 18, no. 19, pp. 3003-3010 2018, DOI: 10.1039/c8lc00434j

[10] T. A. Franke and A. Wixforth, "Microfluidics for Miniaturized Laboratories on a Chip," *ChemPhysChem,* vol. 9, no. 15, pp. 2140-2156 2008, DOI: https://doi.org/10.1002/cphc.200800349

[11] N. Ota, Y. Yalikun, T. Suzuki, S. W. Lee, Y. Hosokawa, K. Goda, and Y. Tanaka, "Enhancement in acoustic focusing of micro and nanoparticles by thinning a microfluidic device," *Royal Society Open Science,* vol. 6, no. 2, p. 181776 2019, DOI: doi:10.1098/rsos.181776

[12] A. Fakhfouri, C. Devendran, D. J. Collins, Y. Ai, and A. Neild, "Virtual membrane for filtration of particles using surface acoustic waves (SAW)," *Lab on a Chip,* vol. 16, no. 18, pp. 3515-3523 2016, DOI: 10.1039/c6lc00590j

[13] S. Zhao, M. Wu, S. Yang, Y. Wu, Y. Gu, C. Chen, J. Ye, Z. Xie, Z. Tian, and H. Bachman, "A disposable acoustofluidic chip for nano/microparticle separation using unidirectional acoustic transducers," *Lab on a Chip,* 2020, DOI: 10.1039/d0lc00106f

[14] Z. Mao, Y. Xie, F. Guo, L. Ren, P. H. Huang, Y. Chen, J. Rufo, F. Costanzo, and T. J. Huang, "Experimental and numerical studies on standing surface acoustic wave microfluidics," (in eng), *Lab on a Chip,* vol. 16, no. 3, pp. 515-24 Feb 7. 2016, DOI: 10.1039/c5lc00707k

[15] X. Ding, Z. Peng, S.-C. S. Lin, M. Geri, S. Li, P. Li, Y. Chen, M. Dao, S. Suresh, and T. J. Huang, "Cell separation using tilted-angle standing surface acoustic waves," *Proceedings of the National Academy of Sciences,* vol. 111, no. 36, pp. 12992-12997 2014, DOI: 10.1073/pnas.1413325111

[16] K. Yosioka and Y. Kawasima, "Acoustic radiation pressure on a compressible sphere," *Acta Acustica united with Acustica,* vol. 5, no. 3, pp. 167-173 1955,

[17] P. Li, Z. Mao, Z. Peng, L. Zhou, Y. Chen, P.-H. Huang, C. I. Truica, J. J. Drabick, W. S. El-Deiry, M. Dao, S. Suresh, and T. J. Huang, "Acoustic separation of circulating tumor cells," *Proceedings of the National Academy of Sciences,* vol. 112, no. 16, pp. 4970-4975 2015, DOI: 10.1073/pnas.1504484112

[18] G. Czerlinski, D. Reid, A. Apostol, K. Bauer, and D. Scarpelli, "Determination of the density of cells from sedimentation studies at 1G," *Journal of Biological Physics,* vol. 15, no. 2, pp. 29-32 1987, DOI: 10.1007/BF01867139

[19] G. Guigas, C. Kalla, and M. Weiss, "The degree of macromolecular crowding in the cytoplasm and nucleoplasm of mammalian cells is conserved," *FEBS letters,* vol. 581, no. 26, pp. 5094-5098 2007, DOI: 10.1016/j.febslet.2007.09.054